Electronic Supplementary Material (ESI) for Physical Chemistry Chemical Physics.

Supporting Information

$Au_{10}Ag_{17}(TPP)_{10}(SR)_6Cl_5$ Nanocluster: Structure, Transformation and the Origin of its Photoluminescence

Along Ma,[a] Jiawei Wang,[a] Jie Kong,[b] Yonggang Ren,[a] Yuxuan Wang,[a] Xiaoshuang Ma,[a] Meng Zhou,[b,*] and Shuxin Wang[a,*]

[a] College of Materials Science and Engineering, Qingdao University of Science and Technology, Qingdao, Shandong 266042, P. R. China

[b] Hefei National Research Center for Physical Sciences at the Microscale, Department of Chemical Physics, University of Science and Technology of China, Hefei, Anhui 230026, P. R. China

*Corresponding authors. E-mail: shuxin_wang@qust.edu.cn (Shuxin Wang), mzhou88@ustc.edu.cn (Meng Zhou);

Notes: The authors declare no competing financial interest.

This Supporting Information includes:

Experimental

Chemicals

All reagents were commercially available and used without further purification. Tetrachloroauric(III) acid ($HAuCl_4 \cdot 3H_2O$, 99.99% metal basis), silver nitrate ($AgNO_3$, 98% metals basis), phenylethyl mercaptan ($HSCH_2CH_2Ph$, 99%), 3,5-bis(trifluoromethyl)thiophenol ($HSPh^{3,5}\text{-}R_2$, R = CF_3, 99%), triphenylphosphine (PPh_3, 98.8%), sodium borohydride ($NaBH_4$, 98%), sodium hexafluoroantimonate ($NaSbF_6$, 98%), triethylamine (Et_3N, 98%), rhodamine b (RhB, 99%), perylene ($C_{20}H_{12}$, 99%), rubrene ($C_{42}H_{28}$, 99%), acetonitrile (CH_3CN, HPLC grade), ethanol (EtOH, HPLC grade), dichloromethane (DCM, HPLC grade), diethyl ether ($C_2H_5OC_2H_5$, HPLC grade), tetrahydrofuran (THF, HPLC grade), 2-methyltetrahydrofuran (2-MeTHF, HPLC grade) and n-hexane (Hex, HPLC grade), were purchased from Sigma-Aldrich.

Synthesis of $Au_{10}Ag_{17}(TPP)_{10}(SR)_6Cl_5$ nanocluster

Typically, $HAuCl_4 \cdot 3H_2O$ (0.20 g/mL, 250 μL, 0.13 mmol) and $AgNO_3$ (25 mg, 0.15 mmol, dissolved in 2 mL of H_2O) were added to the 15 mL of ethanol and 5 mL of CH_2Cl_2 under vigorous stirring. After stirring for 5 min, PPh_3 (200 mg, 0.76 mmol) and $HSPh(CF_3)_2$ (32 μl, 0.18 mmol) were added to the reaction. After 30 min, the reaction solution turned colorless and transparent. Next, a freshly prepared solution of $NaBH_4$ (30 mg, 0.79 mmol, dissolved in 2 mL of H_2O) was added, and the solution gradually changed to dark. The reaction lasted 18 h at room temperature and finally the **$Au_{10}Ag_{17}$** nanocluster was produced (yield ~20 %, Au atom basis). After that, in order to obtain the pure **$Au_{10}Ag_{17}$** nanoclusters, the solution was centrifuged, and the crude product was dissolved in ethanol (50 mL) and stored in a refrigerator (4 °C) for several months. The supernatant was collected by centrifugation. And the crude product was washed with n-hexane three times to get the **$Au_{10}Ag_{17}$** nanocluster. Black, block-shaped crystals were acquired by crystallizing the pure nanoclusters in DCM/Hex (1 : 3) after ~2 weeks at room temperature.

Conversion from $Au_{10}Ag_{17}(TPP)_{10}(SR)_6Cl_5$ nanocluster to $[Au_{12}Ag_{13}(TPP_3)_{10}(PET)_5Cl_2]^{2+}$ nanocluster

The **$Au_{10}Ag_{17}$** (10 mg) and PET (100 μL) were dissolved in 20 mL of CH_2Cl_2 under vigorous stirring. After 3 min, **$Au_{10}Ag_{17}$** were converted into the **$Au_{12}Ag_{13}$** (yield ~30 %, Au atom basis), then CH_3CN was added to stop the reaction. **$Au_{12}Ag_{13}$** was obtained by crystallizing the nanoclusters in DCM/$C_2H_5OC_2H_5$ (1 : 3) after 3 days.

Characterization

Ultraviolet-visible absorption spectra in this study were recorded on a Shanghai Metash UV-8000 spectrophotometer. All samples were dissolved in DCM or 2-MeTHF for spectrum measurements.

The X-ray photoelectron spectroscopy (XPS) measurements were performed on ESCALAB XI+ configured with a monochromated $Al_{K\alpha}$ (1486.8 eV) 150W X-ray source, 0.5 mm circular spot size, a flood gun to counter charging effects, and the analysis chamber base pressure lower than 1 $x10^{-9}$ mbar, data were collected with FAT = 20 eV.

Photoluminescence (PL) spectra of the solutions of clusters were carried out on HITACHI F-4600 PL spectrophotometer. The PLQY of **$Au_{10}Ag_{17}$** was calculated with $Ag_{25}(SPh^{2,4}\text{-}Me_2)_{18}$ (PLQY=0.6%, DCM)

as the reference. And the PLQY of $\mathbf{Au_{12}Ag_{13}}$ was calculated with RhB (PLQY=70%, EtOH) as the reference at room temperature.

Temperature-dependent PL spectra and UV-vis absorption spectra of clusters were carried out on NOVA Laboratory Spectrometer of ideaoptics.

Single-crystal X-ray diffraction (SC-XRD) datas of the $\mathbf{Au_{10}Ag_{17}}$ and $\mathbf{Au_{12}Ag_{13}}$ nanoclusters were collected on a Xtalab Synergy diffractometer at 170 K, using Mo-Kα radiation (λ= 1.54186 Å). With the help of Olex2, the structure was solved with the ShelXT structure solution program.

The fs-TA experiment was performed on a home-built setup based on a commercial amplified Ti:sapphire laser (Coherent, Astrella, 1 KHz, 7 mJ). The ns-TA experiment was performed on a commercial setup (Nano100, Time-Tech Spectra) using the same fs laser as the pump.

Supplementary Figures

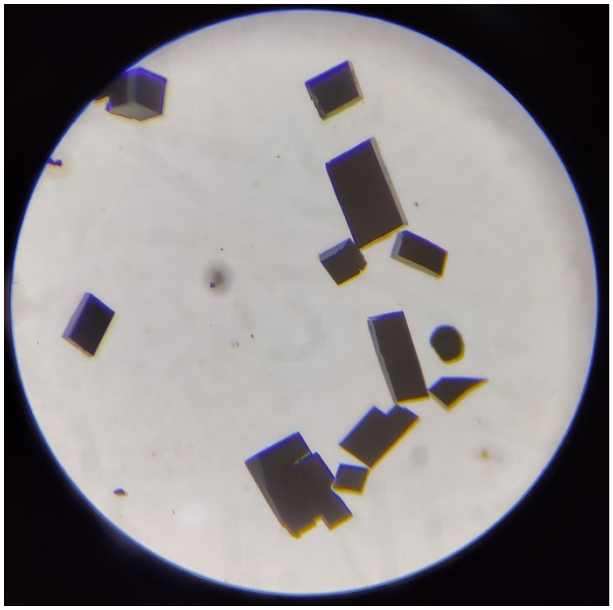

Fig. S1 An optical microscopic image of the single crystals of $\mathbf{Au_{10}Ag_{17}}$ nanoclusters, which are grown by the vapor diffusion of n-hexane into a concentrated CH_2Cl_2 solution of the nanocluster.

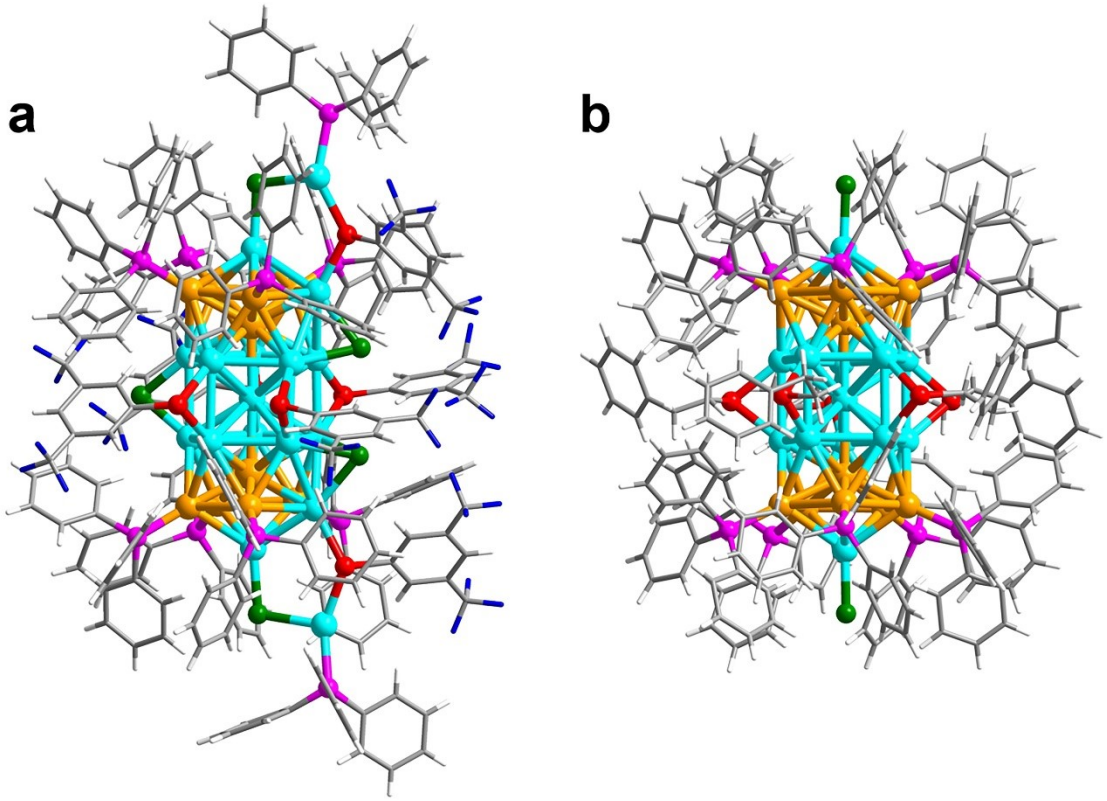

Fig. S2 The overall structure of the $Au_{10}Ag_{17}$ and $Au_{12}Ag_{13}$ nanoclusters. (a) $Au_{10}Ag_{17}$. (b) $Au_{12}Ag_{13}$. Color labels: orange = Au; light blue = Ag; green = Cl; red = S; magenta = P; blue = F; grey = C; white = H.

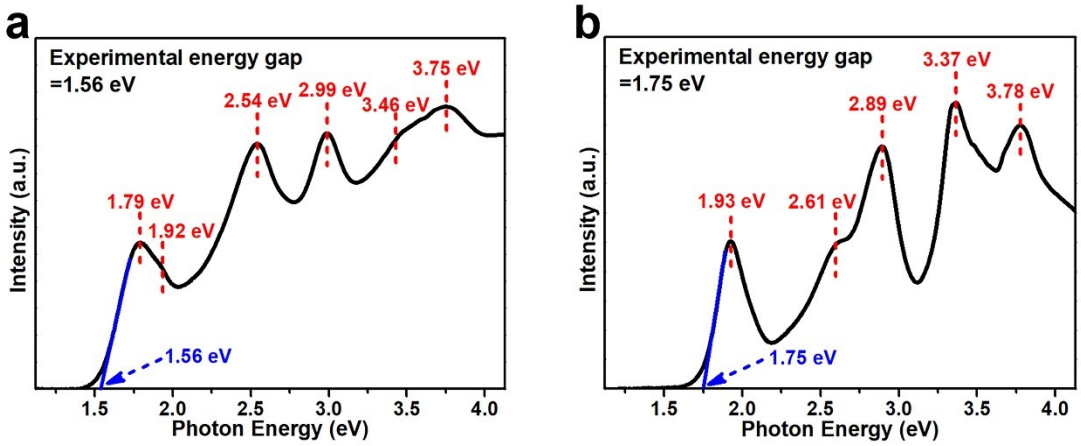

Fig. S3 UV-vis absorption spectra (photon energy scale) of the $Au_{10}Ag_{17}$ and $Au_{12}Ag_{13}$ nanoclusters in CH_2Cl_2. (a) $Au_{10}Ag_{17}$. (b) $Au_{12}Ag_{13}$. The experimental energy gap of the $Au_{10}Ag_{17}$ and $Au_{12}Ag_{13}$ nanoclusters in CH_2Cl_2 was determined as ~1.56 eV and 1.75 eV, respectively.

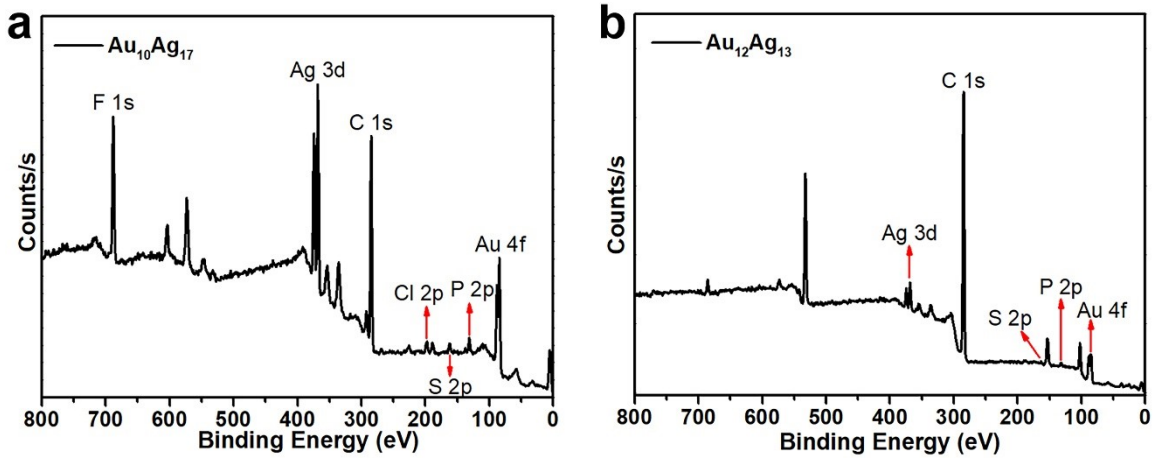

Fig. S4 XPS spectra of the $\mathbf{Au_{10}Ag_{17}}$ and $\mathbf{Au_{12}Ag_{13}}$ nanoclusters. (a) Survey data of $\mathbf{Au_{10}Ag_{17}}$ nanocluster. (b) Survey data of $\mathbf{Au_{12}Ag_{13}}$ nanocluster.

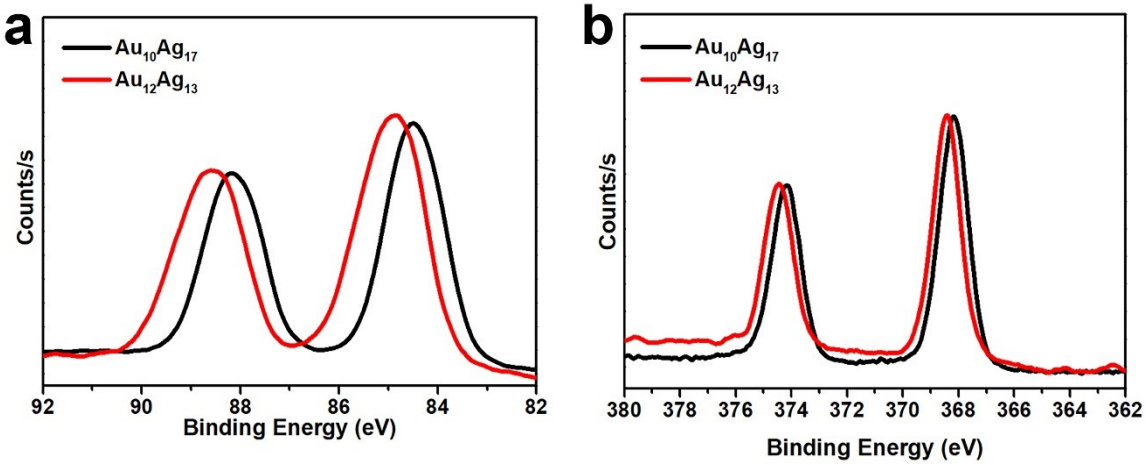

Fig. S5 XPS spectra of the $\mathbf{Au_{10}Ag_{17}}$ and $\mathbf{Au_{12}Ag_{13}}$ nanoclusters. (a) Au 4f. (b) Ag 3d.

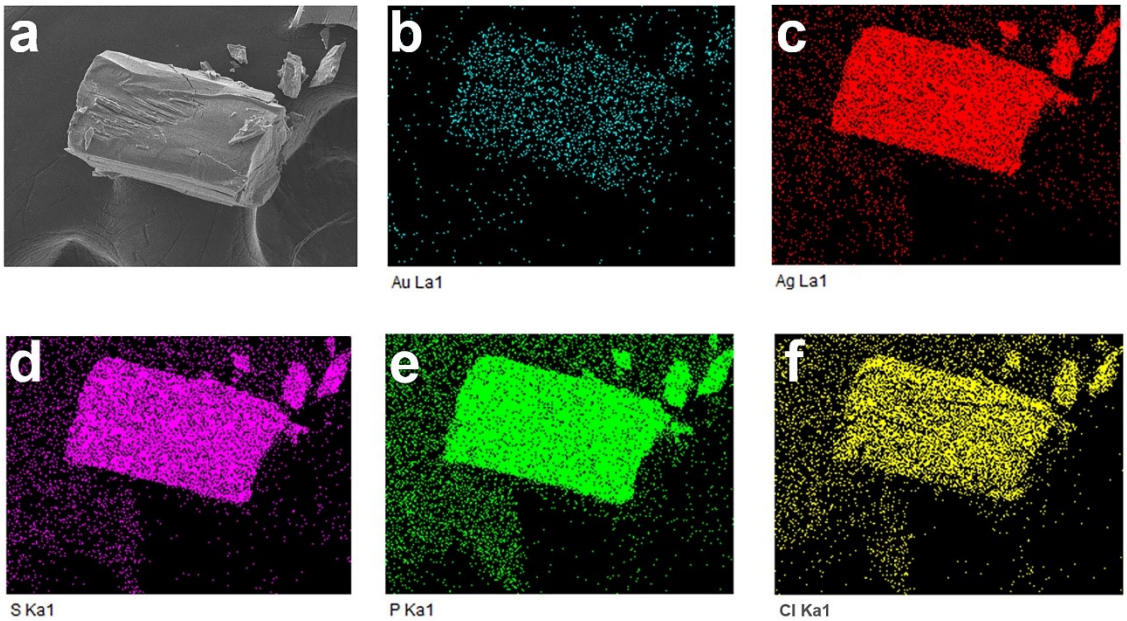

Fig. S6 . (a) SEM image of a small deformed single crystal of $\mathbf{Au_{10}Ag_{17}}$. (b)-(f) Elemental mapping images of Au, Ag, S, P and Cl, respectively.

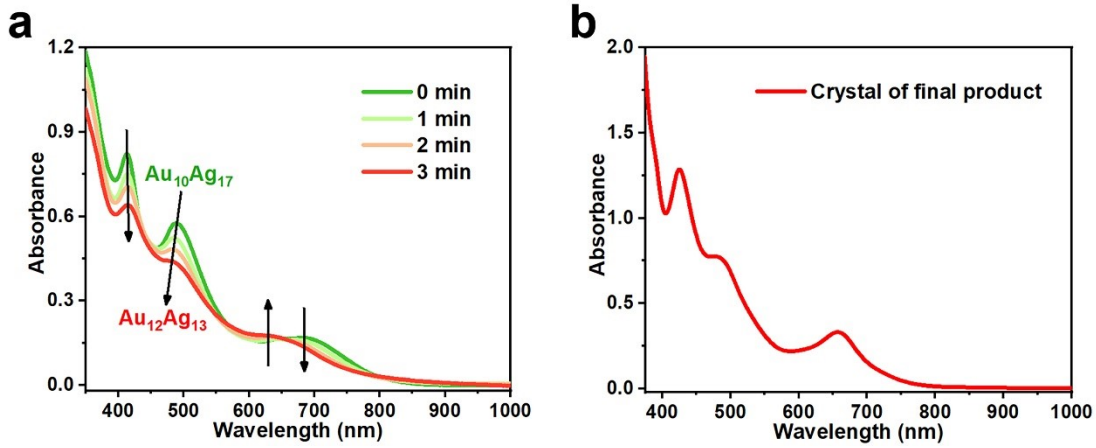

Fig. S7 (a) Time-dependent optical absorptions of the conversion of $\mathbf{Au_{10}Ag_{17}}$ to $\mathbf{Au_{12}Ag_{13}}$. (b) The crystal UV-vis absorption spectrum of final product ($\mathbf{Au_{12}Ag_{13}}$ nanocluster).

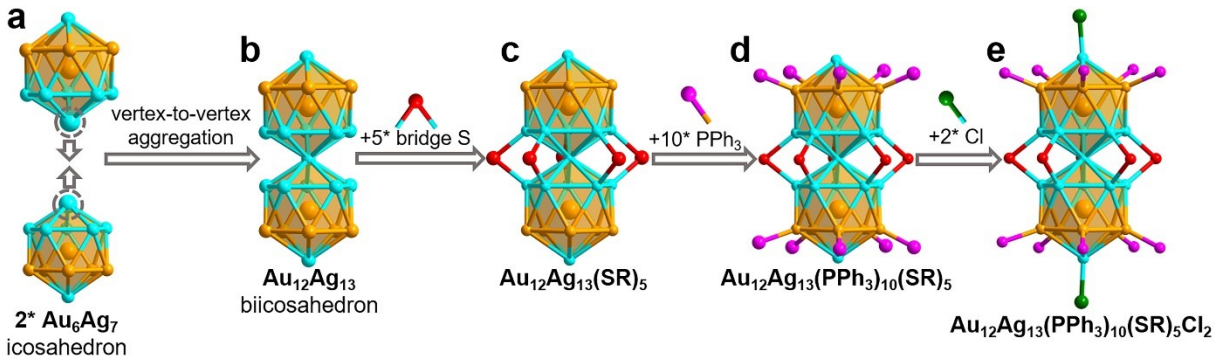

Fig. S8 Structural anatomy of the **$Au_{12}Ag_{13}$** nanocluster. (a) The mono-icosahedral Au_6Ag_7 unit. (b) The biicosahedral $Au_{12}Ag_{13}$ kernel. (c) The $Au_{12}Ag_{13}(SR)_5$ structure with five waist SR ligands. (d) The $Au_{12}Ag_{13}(PPh_3)_{10}(SR)_5$ structure with ten shoulder PPh_3 ligands. (e) The $Au_{12}Ag_{13}(PPh_3)_{10}(SR)_5Cl_2$ with two vertex Cl ligands. Color labels: orange = Au; light blue = Ag; green = Cl; red = S; magenta = P. All C and H atoms are omitted for clarity.

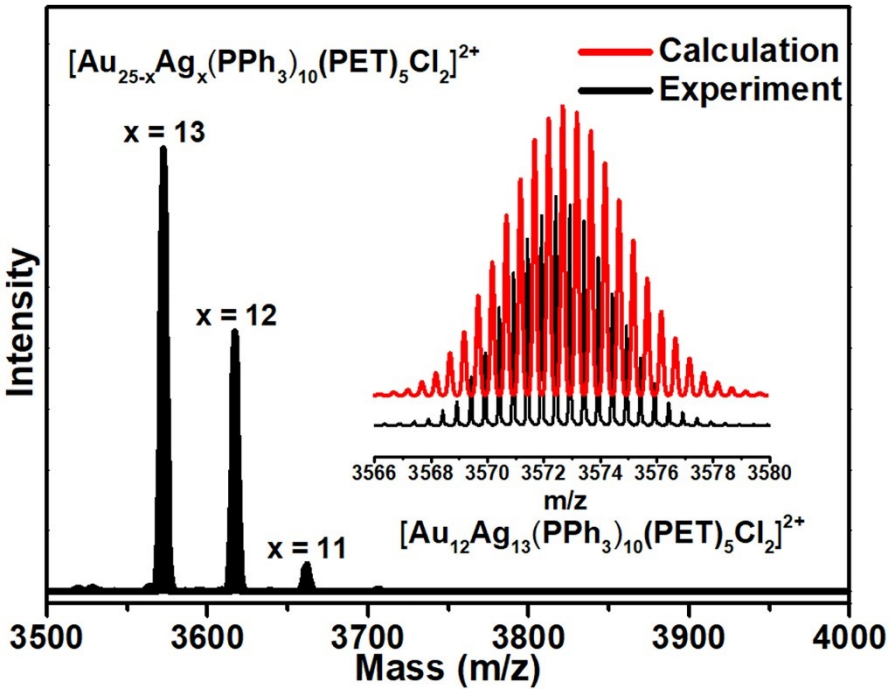

Fig. S9 ESI-MS results of the final product (**$Au_{12}Ag_{13}$** nanocluster).

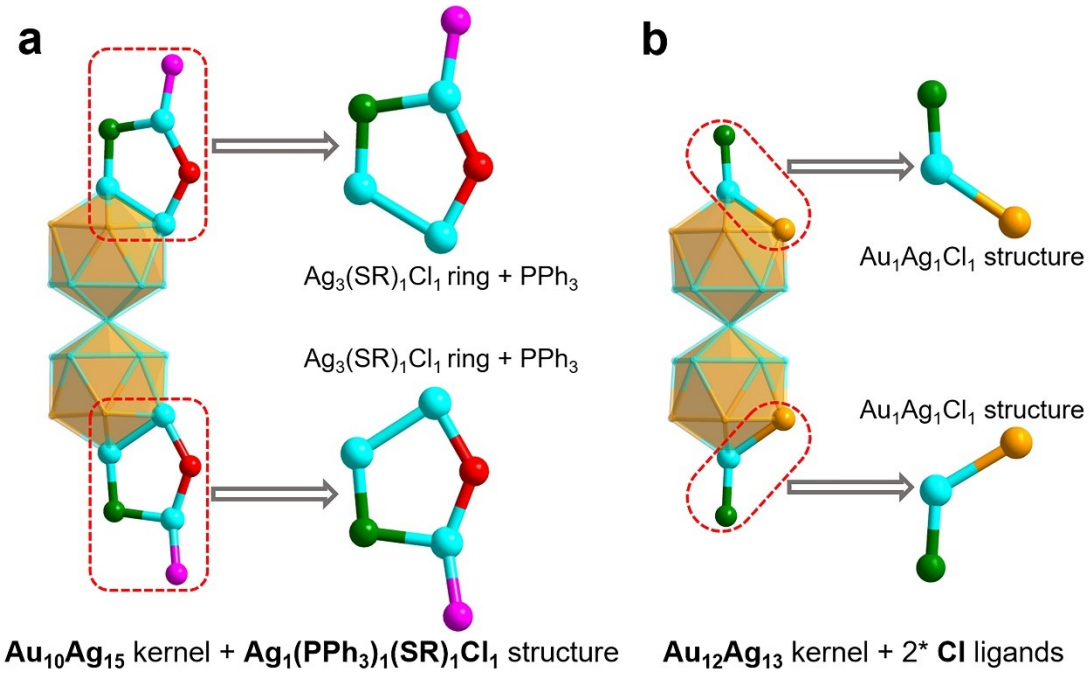

Fig. S10 Different surface structure between vertex Ag and shoulder Ag/Au in the **$Au_{10}Ag_{17}$** and **$Au_{12}Ag_{13}$** nanoclusters. (a) The $Ag_1(PPh_3)_1(SR)_1Cl_1$ surface structure between vertex Ag and shoulder Ag in the **$Au_{10}Ag_{17}$** nanocluster. (b) The $Au_1Ag_1Cl_1$ structure in **$Au_{12}Ag_{13}$** nanocluster. Color labels: orange = Au; light blue = Ag; green = Cl; red = S; magenta = P.

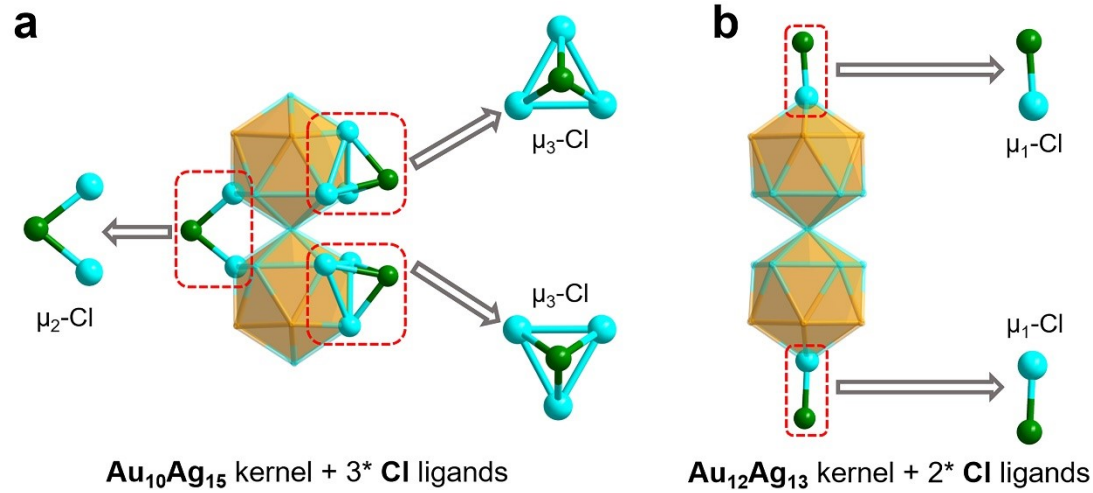

Fig. S11 Bridging mode of Cl in the **$Au_{10}Ag_{17}$** and **$Au_{12}Ag_{13}$** nanoclusters. (a) Bonding between three Cl ligands and the $Au_{10}Ag_{15}$ kernel in **$Au_{10}Ag_{17}$** nanocluster. (b) Bonding between two Cl ligands and the $Au_{12}Ag_{13}$ kernel in **$Au_{12}Ag_{13}$** nanocluster. Color labels: orange = Au; light blue = Ag; green = Cl.

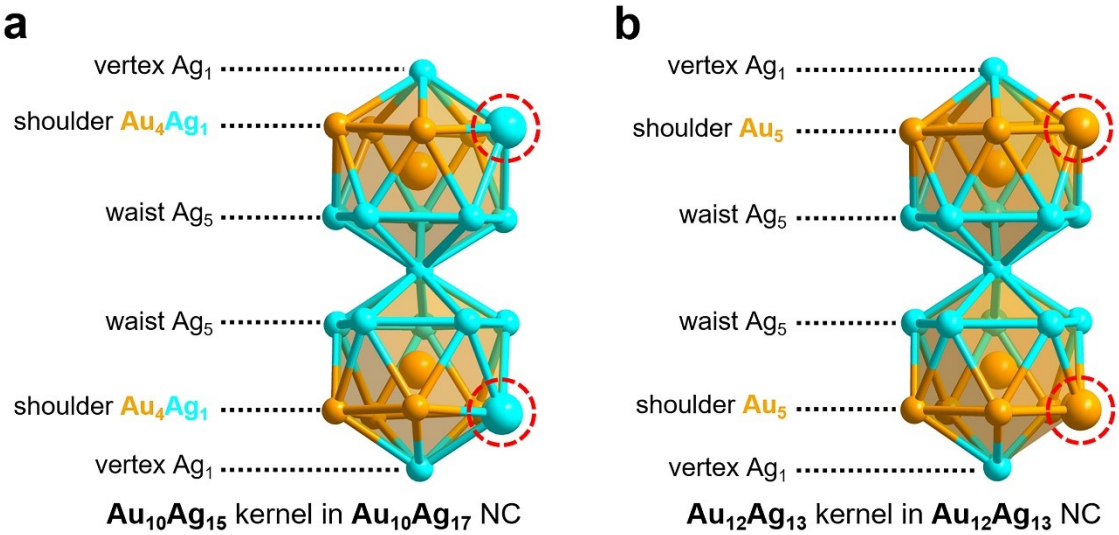

Fig. S12 M_{25} biicosahedral kernel in the **$Au_{10}Ag_{17}$** and **$Au_{12}Ag_{13}$** nanoclusters. (a) $Au_{10}Ag_{15}$ kernel in **$Au_{10}Ag_{17}$** nanocluster. (b) $Au_{12}Ag_{13}$ kernel in **$Au_{12}Ag_{13}$** nanocluster. Color labels: orange = Au; light blue = Ag.

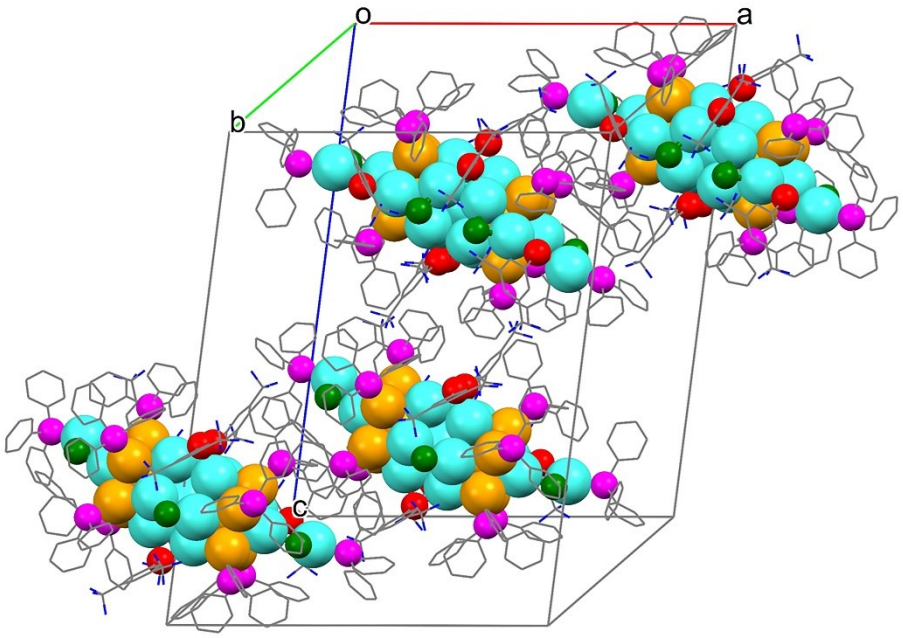

Fig. S13 A unit cell in the **$Au_{10}Ag_{17}$** single crystal. Color labels: orange = Au; light blue = Ag; green = Cl; red = S; magenta = P; blue = F; grey = C. All H atoms are omitted for clarity.

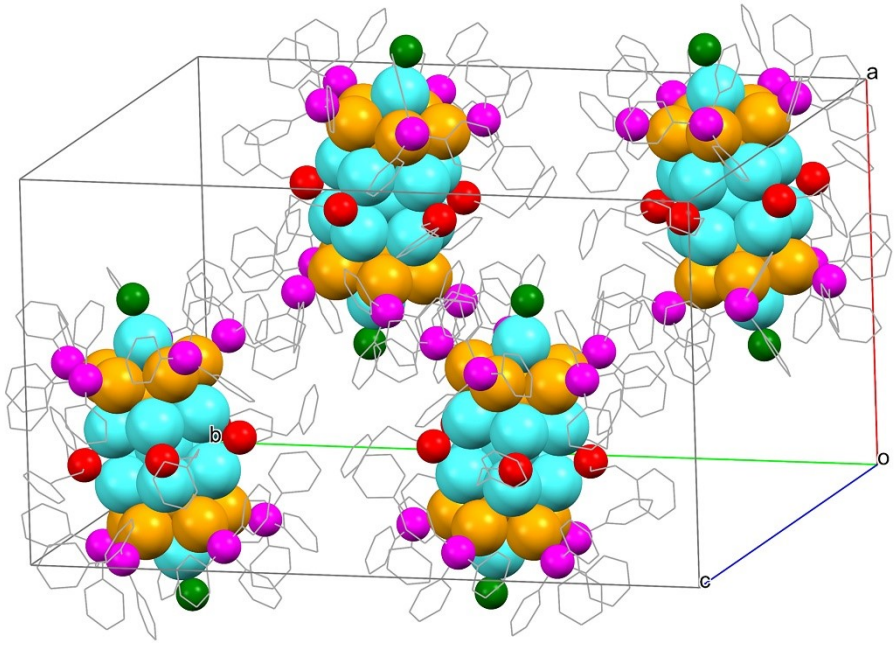

Fig. S14 A unit cell in the $\mathbf{Au_{12}Ag_{13}}$ single crystal. Color labels: orange = Au; light blue = Ag; green = Cl; red = S; magenta = P; grey = C. All H atoms are omitted for clarity.

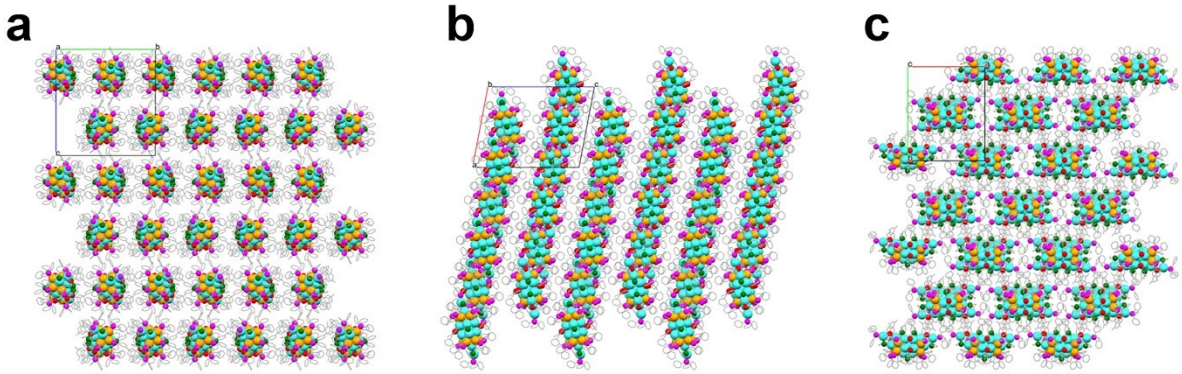

Fig. S15 Packing mode of the $\mathbf{Au_{10}Ag_{17}}$ in the crystal shown. (a) Along the a axis, (b) Along the b axis, (c) Along the c axis. Color labels: orange = Au; light blue = Ag; green = Cl; red = S; magenta = P; grey = C. All H and F atoms are omitted for clarity.

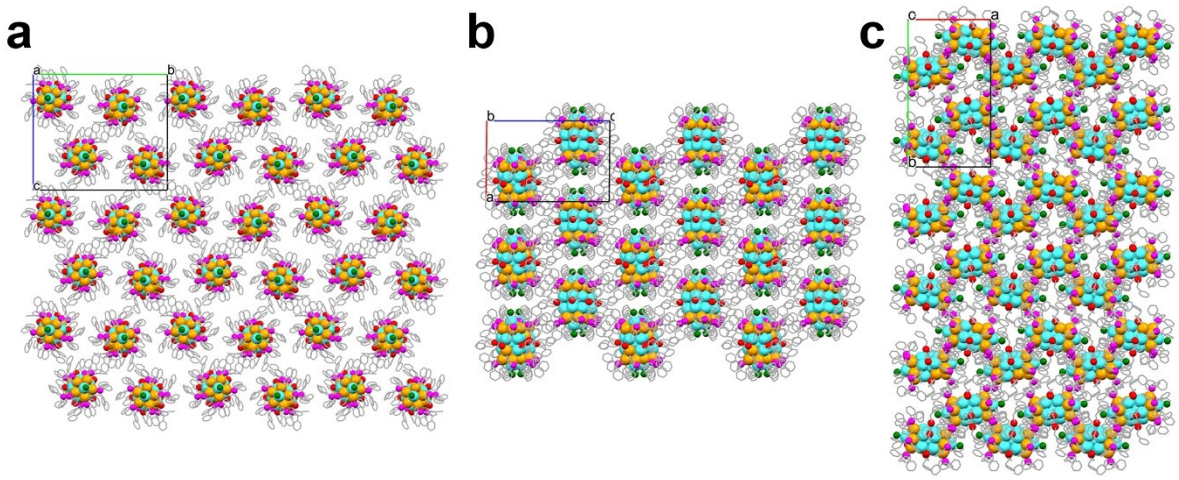

Fig. S16 Packing mode of the $\mathbf{Au_{12}Ag_{13}}$ in the crystal shown. (a) Along the a axis, (b) Along the b axis, (c) Along the c axis. Color labels: orange = Au; light blue = Ag; green = Cl; red = S; magenta = P; grey = C. All H atoms are omitted for clarity.

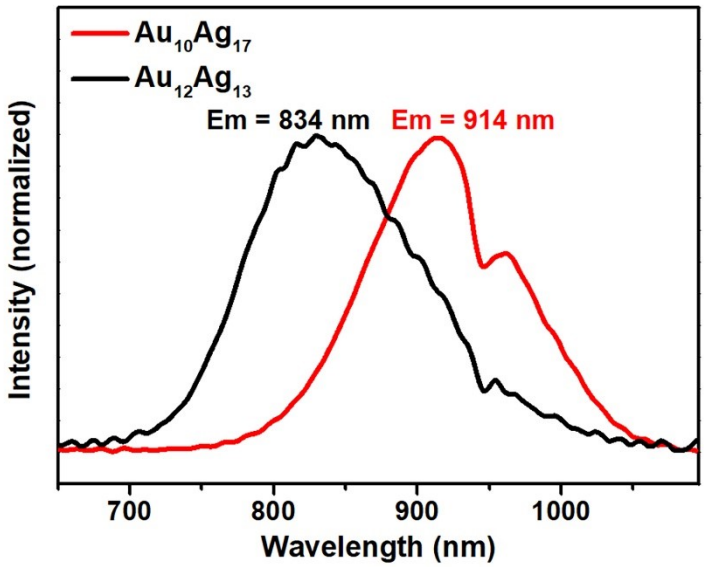

Fig. S17 Normalized photoluminescence spectra of the $\mathbf{Au_{10}Ag_{17}}$ (red, λ_{ex} = 405 nm) and $\mathbf{Au_{12}Ag_{13}}$ (black, λ_{ex} = 405 nm) nanoclusters in the solid state at room temperature.

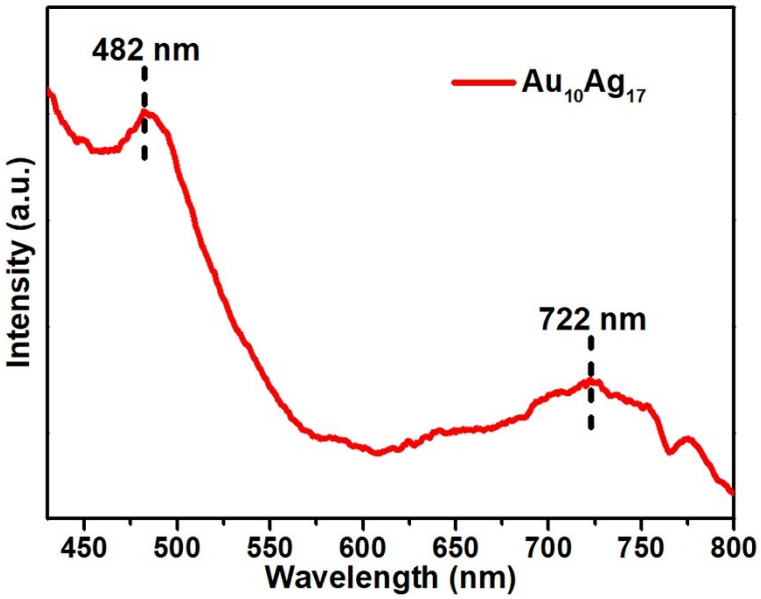

Fig. S18 PL excitation spectra of the $\mathbf{Au_{10}Ag_{17}}$ nanocluster.

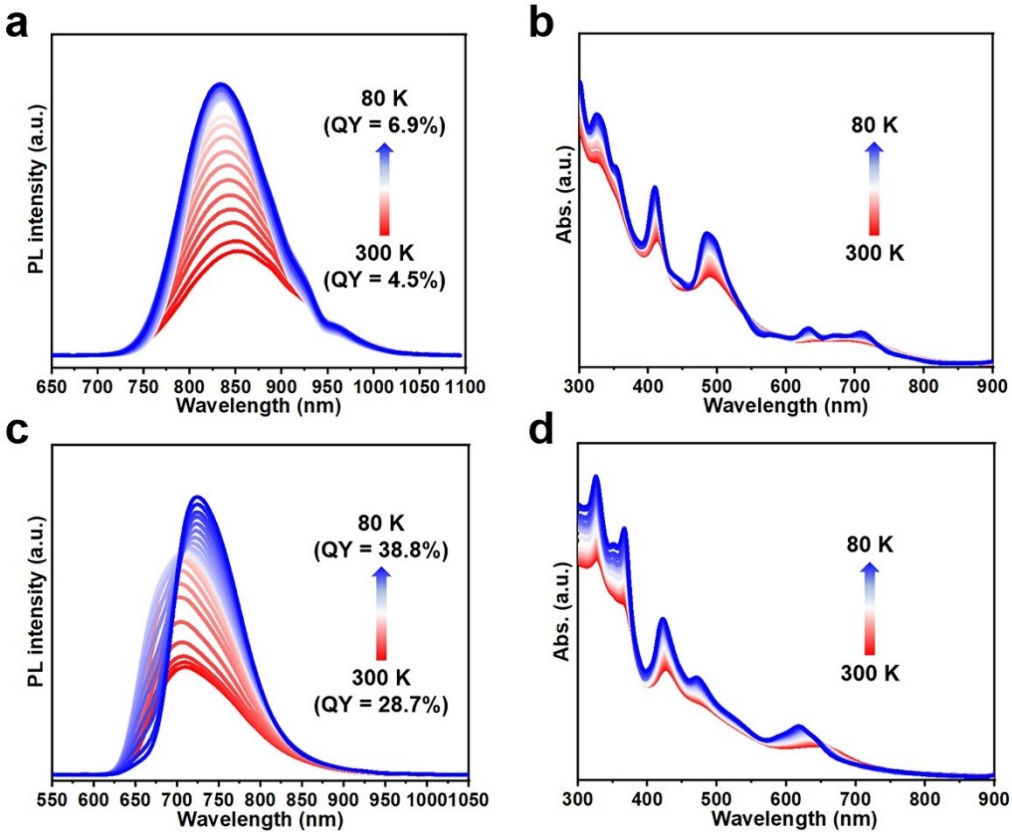

Fig. S19 Temperature-dependent PL spectra and UV-vis absorption spectra of $\mathbf{Au_{10}Ag_{17}}$ and $\mathbf{Au_{12}Ag_{13}}$ nanoclusters in 2-MeTHF (from 300 K to 80 K, monitored per 10 K). (a) Temperature-dependent PL spectra of $\mathbf{Au_{10}Ag_{17}}$ (λ_{ex} = 405 nm, from 300 K to 80 K, monitored per 10 K). (b) Temperature-dependent UV-vis absorption spectra of $\mathbf{Au_{10}Ag_{17}}$. (c) Temperature-dependent PL spectra of $\mathbf{Au_{12}Ag_{13}}$ in 2-MeTHF (λ_{ex} = 423 nm, from 300 K to 80 K, monitored per 10 K). (d) Temperature-dependent UV-vis absorption spectra of

$Au_{12}Ag_{13}$.

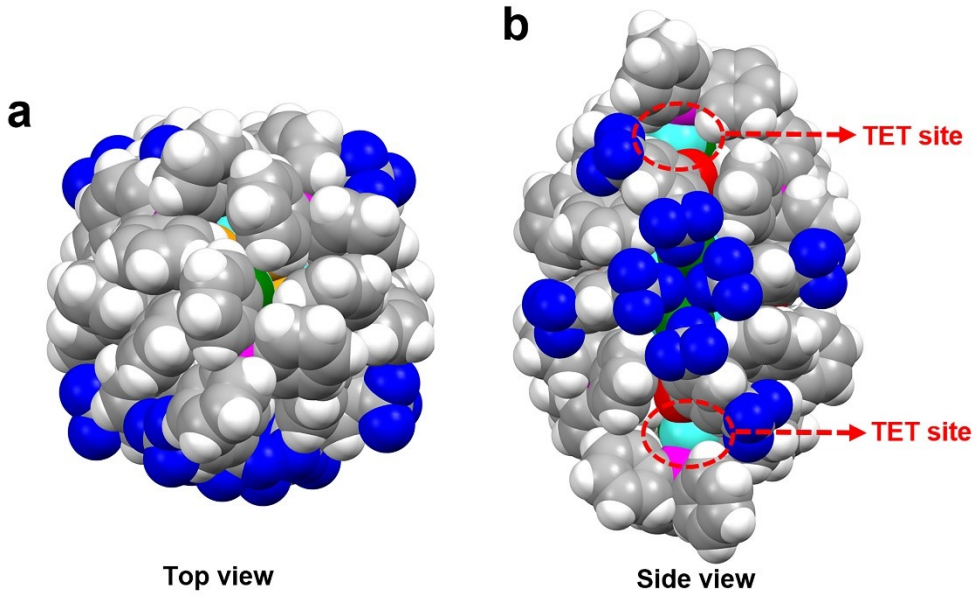

Fig. S20 Geometrical structure (top view and side view) of $Au_{10}Ag_{17}$. Color labels: orange = Au; light blue = Ag; green = Cl; red = S; magenta = P; blue = F; grey = C; white = H.

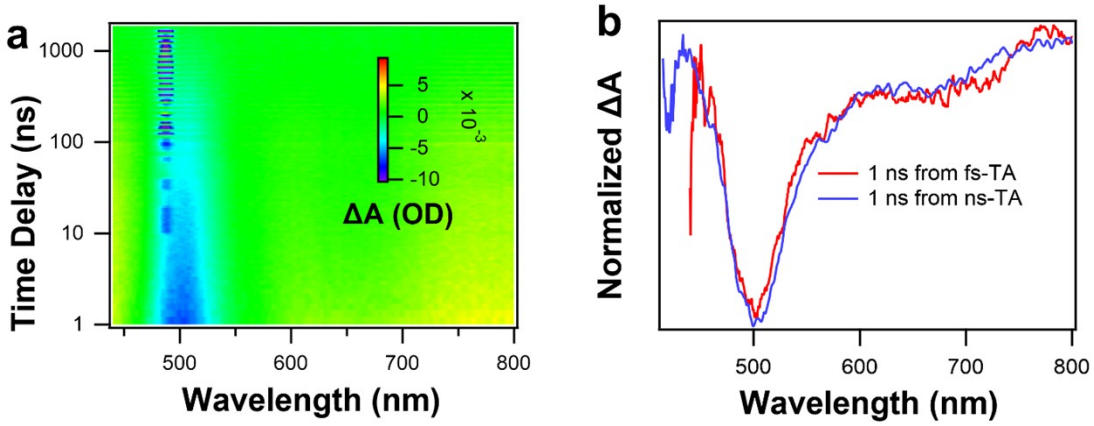

Fig. S21 (a) ns-TA data map with 490 nm ex. (b) Comparison of TA spectra probed at 1 ns obtained from fs-TA and ns-TA measurements.